AFRL-SN-WP-TP-2006-108

MODELING OF TIME-DEPENDENT THERMAL EFFECTS IN Cr^{2+}-DOPED ZINC SELENIDE THIN DISKS

Patrick A. Berry
Kenneth L. Schepler

FEBRUARY 2006

Approved for public release; distribution is unlimited.

STINFO COPY

SENSORS DIRECTORATE
AIR FORCE RESEARCH LABORATORY
AIR FORCE MATERIEL COMMAND
WRIGHT-PATTERSON AIR FORCE BASE, OH 45433-7320

NOTICE

Using Government drawings, specifications, or other data included in this document for any purpose other than Government procurement does not in any way obligate the U.S. Government. The fact that the Government formulated or supplied the drawings, specifications, or other data does not license the holder or any other person or corporation; or convey any rights or permission to manufacture, use, or sell any patented invention that may relate to them.

This report was cleared for public release by the Air Force Research Laboratory Wright Site (AFRL/WS) Public Affairs Office (PAO) and is releasable to the National Technical Information Service (NTIS). It will be available to the general public, including foreign nationals.

PAO Case Number: AFRL/WS 06-0102, 11 Jan. 2006.

THIS TECHNICAL REPORT IS APPROVED FOR PUBLICATION.

//Signature//

KENNETH L. SCHEPLER, Scientist
EO CM Tech Branch, EO Sensor Tech Div
Sensors Directorate

//Signature//

JOSEPH R. KOESTERS, Chief
EO CM Tech Branch, EO Sensor Tech Div
Sensors Directorate

//Signature//

ROBERT D. GAUDETTE, Col, USAF
Chief, EO Sensor Technology Division
Sensors Directorate

This report is published in the interest of scientific and technical information exchange and its publication does not constitute the Government's approval or disapproval of its ideas or findings.

REPORT DOCUMENTATION PAGE

Form Approved
OMB No. 0704-0188

1. REPORT DATE *(DD-MM-YY)*	2. REPORT TYPE	3. DATES COVERED *(From - To)*
February 2006	Conference Paper Postprint	06/01/2005 – 01/30/2006

4. TITLE AND SUBTITLE
MODELING OF TIME-DEPENDENT THERMAL EFFECTS IN Cr^{2+}-DOPED ZINC SELENIDE THIN DISKS

5a. CONTRACT NUMBER
In-house

5b. GRANT NUMBER

5c. PROGRAM ELEMENT NUMBER
61102F

6. AUTHOR(S)
Patrick A. Berry
Kenneth L. Schepler

5d. PROJECT NUMBER
2003

5e. TASK NUMBER
12

5f. WORK UNIT NUMBER
24

7. PERFORMING ORGANIZATION NAME(S) AND ADDRESS(ES)

Electro-Optical Countermeasures Technology Branch (AFRL/SNJW)
Electro-Optical Sensor Technology Division
Sensors Directorate
Air Force Research Laboratory, Air Force Materiel Command
Wright-Patterson AFB, OH 45433-7320

8. PERFORMING ORGANIZATION REPORT NUMBER
AFRL-SN-WP-TP-2006-108

9. SPONSORING/MONITORING AGENCY NAME(S) AND ADDRESS(ES)

Sensors Directorate
Air Force Research Laboratory
Air Force Materiel Command
Wright-Patterson AFB, OH 45433-7320

Air Force Office of Scientific Research (AFOSR)
875 N. Randolph Street
Arlington, VA 22203-1768

10. SPONSORING/MONITORING AGENCY ACRONYM(S)
AFRL-SN-WP

11. SPONSORING/MONITORING AGENCY REPORT NUMBER(S)
AFRL-SN-WP-TP-2006-108

12. DISTRIBUTION/AVAILABILITY STATEMENT
Approved for public release; distribution is unlimited.

13. SUPPLEMENTARY NOTES

This paper contains color.

Author final manuscript. Conference paper postprint of presentation at Photonics West 2006 Conference, published in SPIE Photonics West 2006 Proceedings, Vol. 6100, 61000X-1 (2006).

14. ABSTRACT
We used finite element software to model the time dependence of thermal lensing and temperature rise in a Cr^{2+}-doped zinc selenide thin disk for pulsed pumping. Two cases, chopped cw and Q-switched pumping, were considered. The model agrees well with experimental results for the chopped pumping case but does not directly agree with Q-switched pumping because the time delay between absorption and heat transfer to the host material is not accounted for in our model.

15. SUBJECT TERMS
Lasers, Cr^{2+} laser, infrared, laser thermal factors, lasers, transition metals, zinc compounds

16. SECURITY CLASSIFICATION OF:			17. LIMITATION OF ABSTRACT:	18. NUMBER OF PAGES	19a. NAME OF RESPONSIBLE PERSON (Monitor) / 19b. TELEPHONE NUMBER *(Include Area Code)*
a. REPORT	b. ABSTRACT	c. THIS PAGE			
Unclassified	Unclassified	Unclassified	SAR	16	Kenneth L. Schepler N/A

Standard Form 298 (Rev. 8-98)
Prescribed by ANSI Std. Z39-18

Modeling of time-dependent thermal effects in Cr^{2+}-doped zinc selenide thin disks

Patrick A. Berry* and Kenneth L. Schepler

Air Force Research Laboratory (AFRL/SNJW), 2241 Avionics Circle,
Wright Patterson Air Force Base, OH 45433-7304

ABSTRACT

We used finite element software to model the time dependence of thermal lensing and temperature rise in a Cr^{2+}-doped zinc selenide thin disk for pulsed pumping. Two cases, chopped cw and Q-switched pumping, were considered. The model agrees well with experimental results for the chopped pumping case but does not directly agree with Q-switched pumping because the time delay between absorption and heat transfer to the host material is not accounted for in our model.

Keywords: Laser thermal factors, lasers, transition metals, zinc compounds

1. INTRODUCTION

The mid-IR wavelength region is important for a number of military uses such as remote chemical sensing, infrared countermeasures (IRCM), and target recognition and designation. In addition to military applications, scientific applications such as spectroscopy, environmental sensing, medicine and some manufacturing applications also require mid-IR sources. These applications, along with a lack of suitable existing sources, are driving development of robust, compact solid-state tunable mid-IR laser sources in the 2 to 4 μm wavelength range.

Laser sources consisting of chromium doped into II-VI host materials have the potential to fill many of these requirements. II-VI compounds, consisting of a group II metal and a group VI element, have excellent IR transmission characteristics as well as low phonon vibration frequencies which reduce non-radiative transition rates for optically active transition metal dopants like chromium even at room temperature. In addition, when substituting for a Group II metal, chromium assumes a divalent ionization state which gives it a desirable energy level scheme. These features make II-VI compounds ideal hosts. Divalent chromium has absorption in the 1.6 to 2.3 μm range along with a laser transition in the 2.3 to 3.4 μm range. Chromium II-VI lasers have been demonstrated using a number of host materials such as zinc selenide, cadmium manganese telluride and cadmium selenide.[1, 2, 3]

The development and widespread use of chromium lasers has long been hampered by the problem of thermal lensing. Thermal lensing occurs when variations in the refractive index (which is a function of temperature) are induced by absorption of laser pump power converted into heat. Heat is generated either through the quantum defect or from non-radiative losses. Thermal gradients across the material alter the phase profile of light passing through the material and effectively act as a lens. This can cause laser cavity instability as well as material damage from focusing at high powers.

The goal of this research was to develop a modeling system that could be used to gain an understanding of the time-dependence of thermal lensing as well as to help expedite the development of better laser designs. With this in mind, it was important to not only construct models with varying time-dependent variables but to also study the effects of variations in the ancillary model parameters. These extra steps were needed to prevent systematic errors inherent in the modeling assumptions from affecting the results and to establish a baseline model from which the proposed designs can be constructed.

* patrick.berry@wpafb.af.mil; phone (937) 904-9663

2. Methodology

2.1 General assumptions

To simplify the modeling process, certain assumptions were made. The laser source was assumed to be uniformly absorbed along the depth of the laser sample. This is not strictly true unless the thickness is small in comparison to the 1/e absorption depth: however multiple back and forth passes tend to even out absorption at different sample depths and the experimental resonator we modeled used a 16-pass setup making absorption quite uniform with depth. Also, heat sinking was assumed to be through perfect heat sinks that maintained a constant temperature on their surface. Lastly, conductive cooling by air was neglected such that all non-heat sink surfaces were considered to be insulating.

The pump beam was assumed to have a Gaussian transverse beam profile. This beam would be of the form in (1), where x_o and y_o define the center point of the beam, n is the Gaussian order, and σ is the beam radius at which the value of the function drops to $1/e^2$. The Gaussian order, *n*, could be varied to study the effects of different beam profiles, but was kept at unity for this research.

$$f_n(x,y) = \exp\left[-\frac{2\left((x-x_0)^2+(y-y_0)^2\right)^n}{\left(\sigma^2\right)^n}\right] \tag{1}$$

2.2 Model Construction

The models were constructed using FemLab® 3.0a, version number 3.0.0.228. The first step in the model construction process was to create the model geometry using the program's CAD interface. In this step it is important to faithfully recreate the important elements of the design while minimizing the extraneous details. This step is important due to the fact that the complexity of the model and therefore the amount of time and memory required in solving the model are directly related to the size of the model and the number of surfaces.

2.2.1 Model design

A simple common laser design, the face-cooled thin disk, was simplified to consist of the laser material and a heat sink. Due to the general assumption of perfect heat sinks, the only part of the heat sink that needed to be included was the surface that was in direct contact with the laser material or window. To illustrate this, Figure 1 shows how the face-cooled thin disk design was 'translated' into the model geometry.

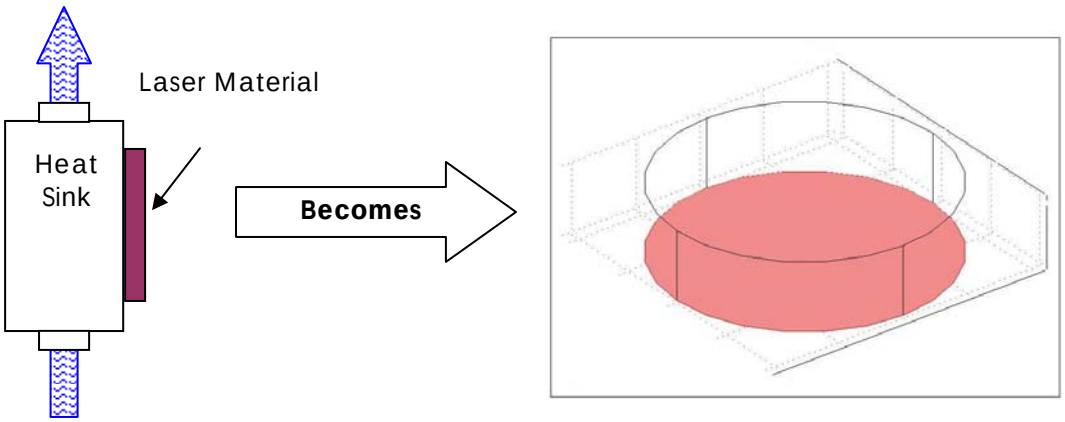

Figure 1: Basic face cooled design translation to model geometry

Once the model geometry was established, boundary conditions and subdomain material parameters were set according to the material properties of the system. These parameters include the important physical properties of the host material, zinc selenide. The subdomain settings also include the heat source *Q*. This is an extremely important parameter as it not only includes the beam profile from above but also the time dependence of the pump beam.

2.2.2 Time-dependent pump algorithm

A method for simulating periodic pumping by a laser source was developed for use in the heat source. The variable *t* is available for use with the time-dependent solver and can be used to create a periodic square wave pulse. This function had to have the value of 1 when the pump laser is on and 0 when it is off. The simplest method to create a square wave was to use logic functions to turn the power on and off. However, solutions generated with this method were found to be extremely inconsistent due to discontinuities of first derivates at the on/off transition times. A better way to create a periodic square wave was through the use of a smoothed step function known as a smoothed Heaviside function. This function, while still essentially the unit step function (x >= 0), is smoothed at the step allowing it to have a first derivative at that point.

The Heaviside function is not a periodic function however, so it needed to operate on a periodic function to achieve the desired pulse train. To understand the algorithm better, it is necessary to look at how a Heaviside function would behave when operating on a periodic function such as a sine wave (Figure 2a). The Heaviside function will then turn on when sin ($2\pi t/T$) >= 0 and off when sin ($2\pi t/T$) < 0 (Figure 2b) where *T* is the period of the sine function. This produces a square wave pulse with a 50% duty cycle because a sine function spends 50% of the time above 0 and 50% below.

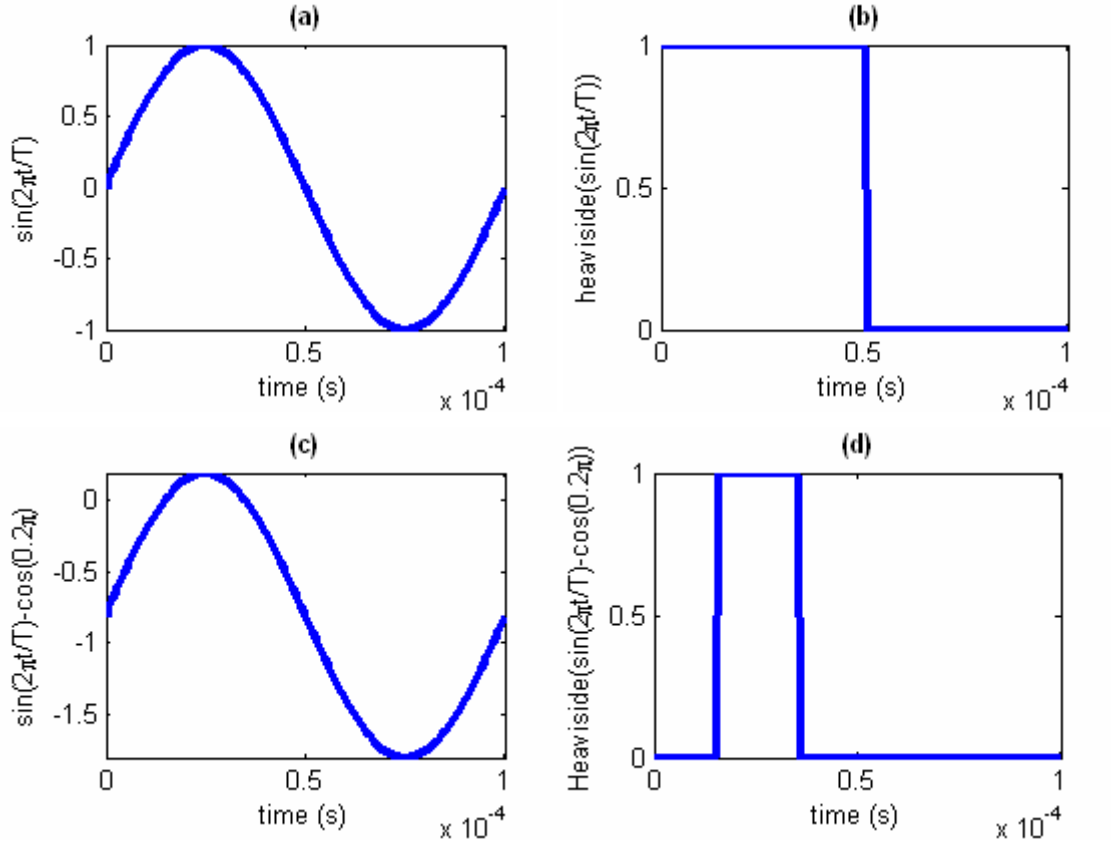

Figure 2: Generation of a time dependent square wave. (a) sine function, (b) 50% duty cycle smoothed Heaviside function, (c) sine function offset by cos (0.2π) = 0.628, (d) 20% duty cycle smoothed Heaviside function.

To model a square wave pulse with a different duty cycle, the sine function that the Heaviside function operates on must be shifted up or down by an offset so that it spends the desired duty cycle above zero. To

determine the correct amount of offset, we simply take the value of a cosine at the desired pulse width. For example, if we want a 20% duty cycle we shift the sine function by cos (0.2π) (Figure 2c). This produces the following square wave pulse with a 20% duty cycle (Figure 2d). Note that the pulse is centered around the π/2 point. This algorithm can be repeated indefinitely to produce a time-dependent pulse train. The algorithm used in the software combines the spatial configuration of the beam with the temporal configuration.

The other important parameter in the pump algorithm is the input power. Care must be taken in determining the power per pulse in a time-dependent algorithm. The software itself ensures that the correct amount of power is available to each time increment in the run. That is, if the power input is set to one watt and the minimum time increment is 1 μs, then the software provides 1 μW to each time increment. Once the pump algorithm acts, this power will either be put into the material or not, thus the peak power is always the same but the average power will depend on duty cycle. This is the analog of a chopped pump beam where a constant amount of CW pump power is chopped to achieve a quasi-CW modulated pump beam.

If the goal is to model a Q-switched pump the average power is generally the same (as long as 1/PRF is less than the relaxation lifetime of the pumping laser) but the peak pump power depends on PRF. Of note in this case is the fact that most Q-switched pump lasers used to pump Cr^{2+} lasers have a pulse width of 100 ns or less which is much smaller than the smallest practical time increment in our modeling program. We have approximated Q-switched pumping in our model by keeping average power constant, using a constant low duty cycle, and varying PRF. A hybrid system with a fixed average power and variable duty-cycle is also possible in theory but difficult to produce in practice.

2.2.3 Minimum time increment

The FemLab® time dependent solver attempts to find a solution at discrete time increments throughout the total time period. The time increment chosen by the user should strike a balance between model accuracy and solution time required. It should also fully resolve the pulses in the pump algorithm. Time increment variations of 10, 5, 2 and 1 μs were modeled for a 10-kHz PRF and 15% duty cycle in order to find the optimal time increment setting. The smallest time increment feasible due to time and memory constraints was 1 μs. Modeling results for larger time increments were inconsistent throughout the model runs but converged on the 1 μs results. This indicated that 1 μs was the optimal time increment to use for all models.

Due to time and memory constraints, it is difficult to run a 1-μs time increment model for 8 ms or longer total time. It would be useful to be able to model longer total time periods by modeling shorter, discrete time periods. The last solution of the previous run would be used as the initial condition for the next model with the results merged into a continuous solution. The comparison of a continuous 8-ms model to two discrete 4-ms models showed that this method is acceptable as the differences in results between the two methods were negligible in comparison to the modeled values. The 1-μs time increment model was also run for 16 ms to see how closely the temperatures approached an asymptote. At 8 ms, the z-average temperature rise (defined as the average temperature rise over a line through the depth of the sample in the propagation (z) direction) is within 0.2 K of the value at 16 ms. This difference is less than 5% of the z-average temperature rise. This number is also within 5% of the steady state average temperature rise of 9.3 K. This confirmed that the maximum total time needed to run the models to achieve asymptotic behavior is 8 ms.

2.2.4 Determination of ancillary parameter values

The goal of the time dependent modeling is to study the effects of different pulse repetition frequencies (PRFs) and duty cycle on both the magnitude of thermal lensing and the overall average temperature rise in the laser material. There are a large number of parameters in models such as this (geometry, time increment, mesh size, etc) and all of them except for PRF and duty cycle must be kept constant from run to run in order to make valid comparisons. A large portion of the modeling work involved determination of appropriate values for these ancillary parameters. The optimal value is one which produces accurate and precise results while still allowing for reasonable solution times.

In previous work, the maximum portion of the laser material geometry that needed to be included in the simulation was determined.[4] It was postulated that areas of the model farther from the center than approximately twice the pump beam radius would be irrelevant to the model solution and could thus be excluded. A set of basic face cooled models (modeled as parallelepipeds for simplicity) was constructed where the x and y dimensions varied from 2 mm to 8 mm while the pump beam σ (see eq. (1)) was 0.4 mm. The thermal lensing power was found to not vary significantly in this range with size and 4-mm sides produced an upper bound on thermal lensing power and maximum average temperature rise. From these models, it was determined that the 4-mm *x* and *y* size was optimal.

Due to limited computer memory and CPU resources, it was desirable to run the models with as few degrees of freedom (a measure of the model complexity) as possible without sacrificing model quality. To insure that model complexity was not lowered to the point of affecting the results, the standard 4-mm model was run at varying degrees of freedom. The results showed that the thermal lensing power and maximum average temperature rise leveled off quickly and that as long as some reasonable mesh size was chosen, the results would be acceptable. With this software package, solution time was not the main impediment, memory consumption was. The most complex model that available 1 GB RAM computers could run was about 220000 degrees of freedom due to memory allocation issues.

Once the appropriate x-y dimensions and model mesh complexity were established, the geometry of the sample itself was studied. Due to symmetry properties, it was beneficial to use thin cylinders instead of parallelepipeds in the models. A 4-mm diameter cylinder was compared to the 4-mm by 4-mm parallelepiped to gauge any differences. Modeling showed that differences in thermal lensing power and maximum average temperature rise between the disk and parallelepiped were two orders of magnitude smaller than the lensing power itself. Thus the difference between the disk and parallelepiped geometries was negligible when looking at thermal lensing power and maximum average temperature rise.

3. Model Results and Analysis

Once the geometric models were constructed and configured as required, the finite element solver was initiated. After a temperature solution for each mesh point was determined for every time increment, the raw temperature data needed to be processed into a more useful form. In this research, we were interested in two types of temperature information. The maximum z-average temperature rise in the laser material has an effect on the fluorescence lifetime while the radial gradient of the z-average temperature is an indication of the magnitude of the thermal lensing. To obtain the z-average temperature, the data for each time increment must be exported and then z-averaged. The radial temperature gradient is important because of the high thermo-optic coefficient of the laser material. As temperature increases, so does the refractive index which means that a temperature gradient will produce an effective quadratic thermal lens. The power of the thermal lens is related to how sharply the gradient peaks. The pump cycle has several interesting times at which the thermal gradient could be measured. These would be mid-way through the pulse, at the peak of the pulse, mid-way through the rest portion of the cycle and just prior to the pulse starting. In this case, because lasing will start at the beginning of the pump pulse, that is where we measured the radial temperature gradient.

As mentioned in a previous section, most pulsed lasers fall into one of two categories. Lasers we will refer to as chopped lasers have a fixed peak power and an average power which varies with duty cycle, all of which are mostly independent of PRF. Lasers we will refer to as Q-switched lasers have a fixed average power, a fixed pulse width and a peak power and duty cycle which vary with PRF. Another category of laser which can be modeled is a hybrid system where the average power is fixed as in the Q-switched case, but the pulse width varies with the duty cycle as in the chopped case.

In our modeling calculations below we assumed 1 W of cw pump power; other powers can be considered by remembering that temperature rise and thermal lensing power scale linearly with pump power. We also assumed a 1-mm thick disk 4 mm in diameter which absorbed all pump power.

3.1 Chopped lasers

In a chopped laser, the peak power is fixed, the average power is determined by the duty cycle and both are independent of the PRF. CW operation corresponds to 1 W peak and average power while 25% duty cycle, for example, is 1 W peak power and 0.25 W average power. For a 1-kHz PRF at varying duty cycles, the

z-average temperature at the center point can be seen in Figure 3. Note that the temperature rise does not completely return to the baseline between pulses but the average temperature does reach an asymptotic value after about 8 ms of pumping. All duty cycles other than cw operation show a saw-tooth $(1-\exp(-t/\tau))$ rise and $(\exp(-t/\tau))$ decay at all times where τ is the relaxation lifetime. Also note that just 1 W cw can result in a 9 K temperature increase; multiple-watt pumping could easily reach temperatures where nonradiative relaxation would become severe.

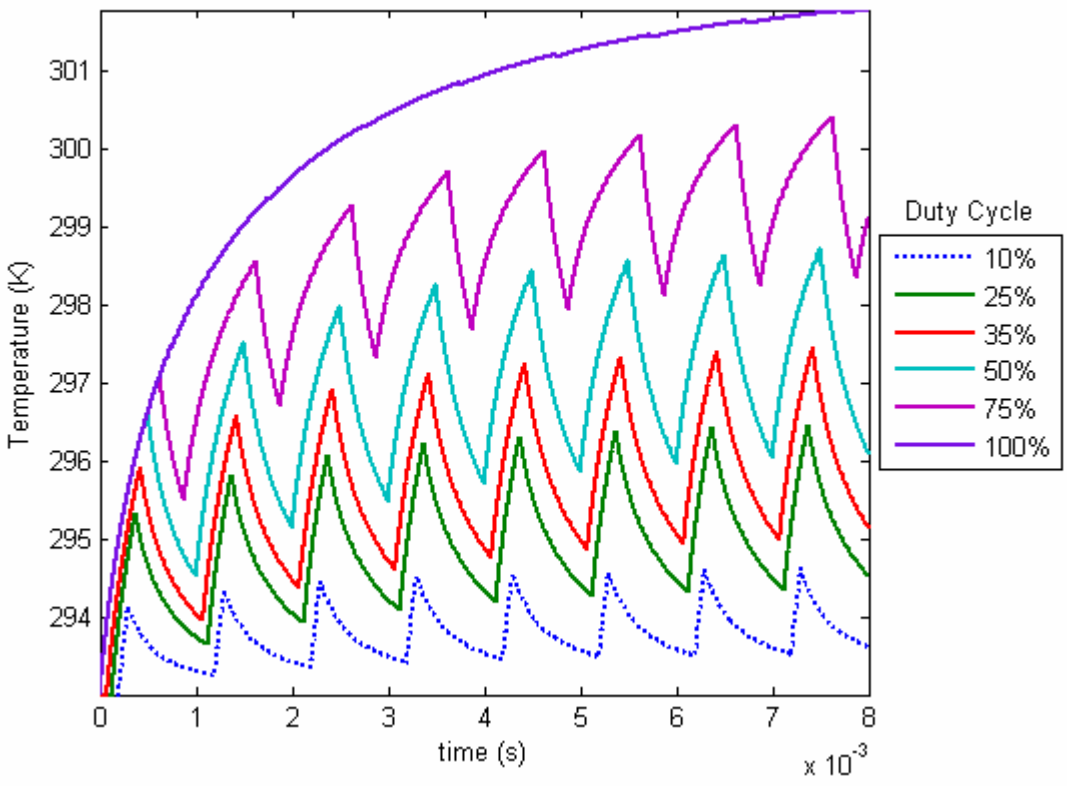

Figure 3: Center point z-average temperature for 1 kHz PRF at varying duty cycles.

The radial thermal profiles for 1 kHz PRF and varying duty cycles are shown in Figure 4. Table 1 shows calculations of thermal lensing power for the different duty cycles. Obviously, thermal lensing should increase with duty cycle (more average power); in fact, it increases quadratically with duty cycle due to increased pump power and decreased time to cool.

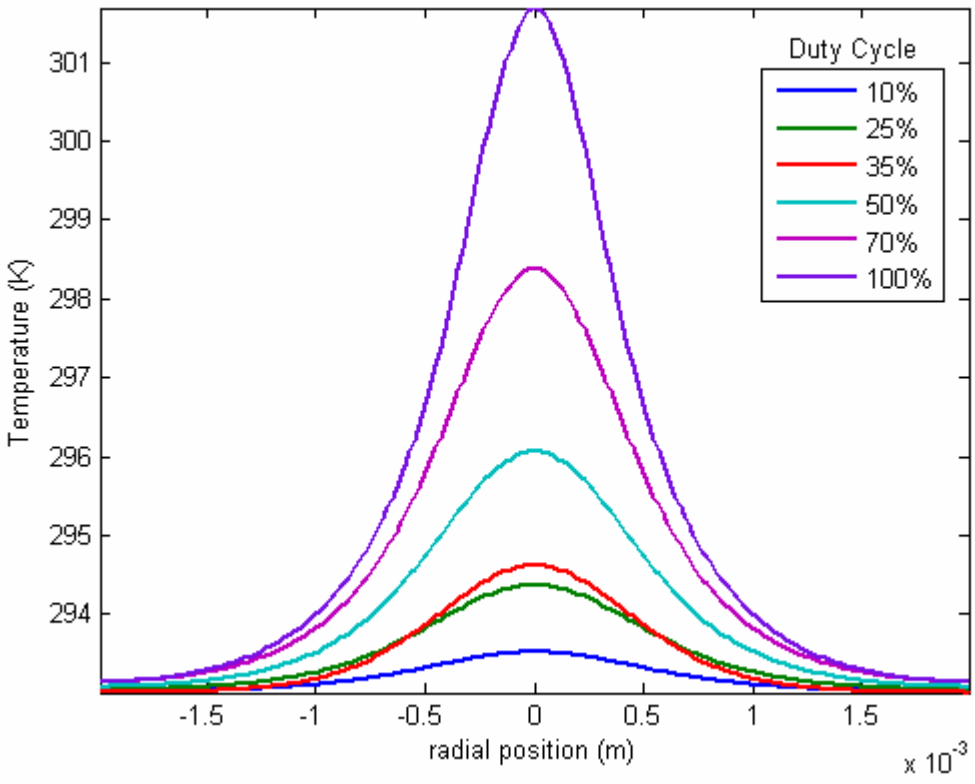

Figure 4: Radial temperature gradient for 1 kHz PRF at varying duty cycles

Table 1: Thermal Lensing Power at 1 kHz PRF, 1 W peak power

Duty cycle (%)	Thermal lens power (m^{-1})
10	0.23
25	0.63
35	0.88
50	1.55
75	3.06
100	6.00

These modeling results predict that lower duty cycles should better support lasing through lower temperatures and lower thermal lensing. This is supported experimentally as seen by the results in Figure 5.[5] At low duty cycles the laser output power slope efficiency remained linear for all average pump powers up to 5 watts. However, the high duty cycle results showed rollover, i.e. reduced slope efficiency above 4.5 W average pump power for 50% duty cycle and above 3.7 W for 100% duty cycle operation. The threshold for rollover is not simply a function of average power because the pump-off times allow the laser material temperatures to cool below the cw average. The decrease in slope efficiency with increasing duty cycle is likely due to the increased average temperature of the sample thus reducing Cr^{2+} energy storage time. The onset of rollover is likely to be due to onset of resonator instability from thermal lensing.

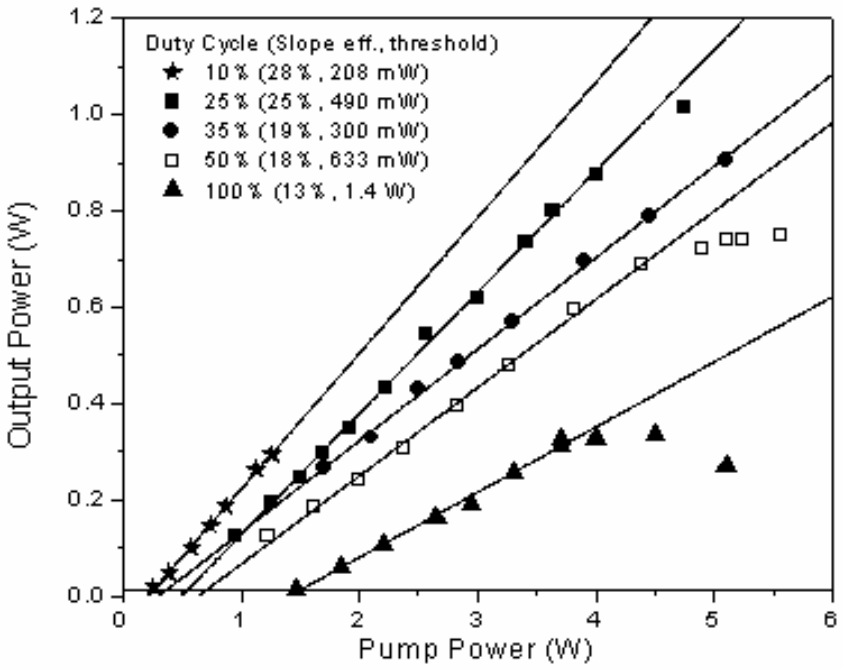

Figure 5: Experimental results for 1 kHz PRF chopped laser with varying duty cycles. Pump power is average power.

3.2 Q-switched Lasers

In a system where the average power and duty cycle are fixed, variations in PRF have little effect on the overall time-average temperature at the center of the material. This is because, over a period of time which is large with respect to the pulse period, the same amount of heat is being put into the laser with the same relative amount of rest time (due to the fixed duty cycle). Figure 6 shows the z-average temperature for 15% duty cycle pumping and varying repetition rate. The model implicitly assumes instantaneous heating with absorption of pump power. It shows that during the pumping time (which is when gain induced Cr^{2+} lasing would be occurring), the average temperature goes higher as the repetition rate decreases. This contradicts the experimental observation that average Cr^{2+} output power is constant with increasing PRF until it approaches 10 kHz and then output declines. However, pumped Cr^{2+} ions do not immediately transfer their stored energy to the crystal lattice; either stimulated emission or transition back to the ground state must occur. Thus the temperatures at the beginning of the pumping are likely to be more representative of the temperature during lasing for the Q-switched case. In that case, the minimum temperature increases with PRF reaching the cw limit as PRF goes to infinity.

The radial temperature gradients were extracted at the low temperature points of each PRF cycle in Figure 6 at times when the average temperature was close to steady state. This is based on the assumption that thermal lensing effects were most important at the beginning of the pump cycle. These gradients can be seen in Figure 7 and the calculated thermal lens powers associated with them are listed in Table 2.

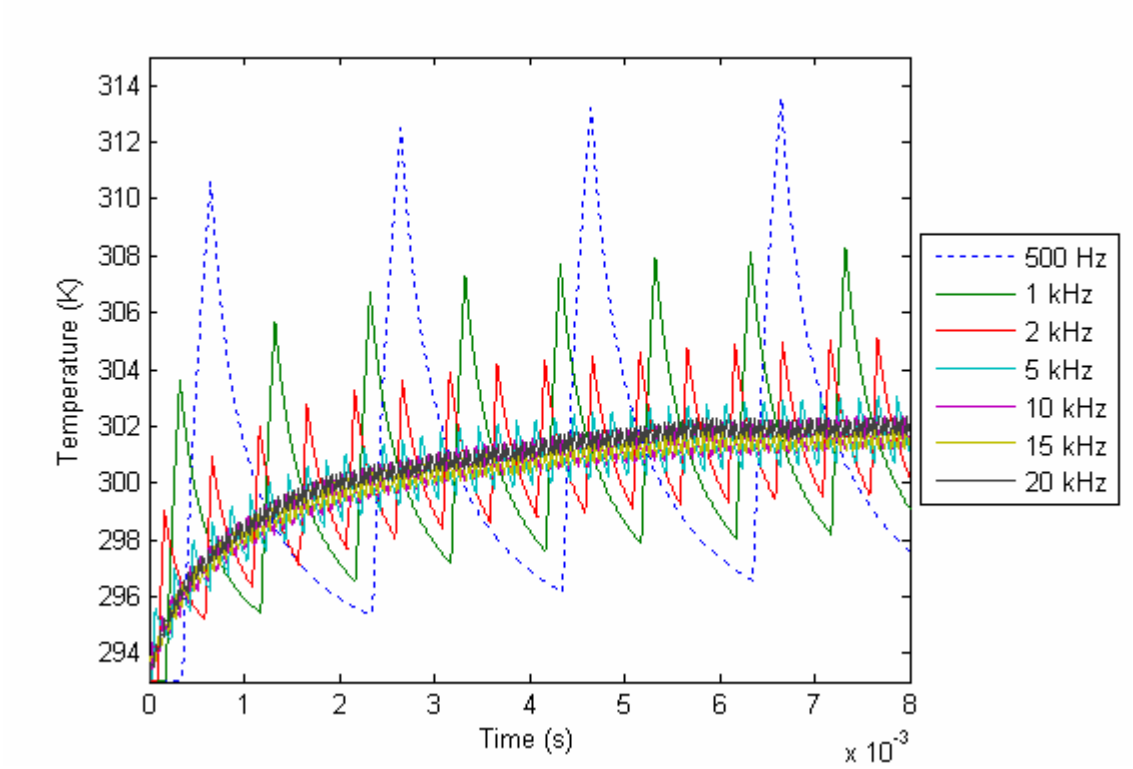

Figure 6: Center point z-average temperature for 15% duty cycle with varying PRF

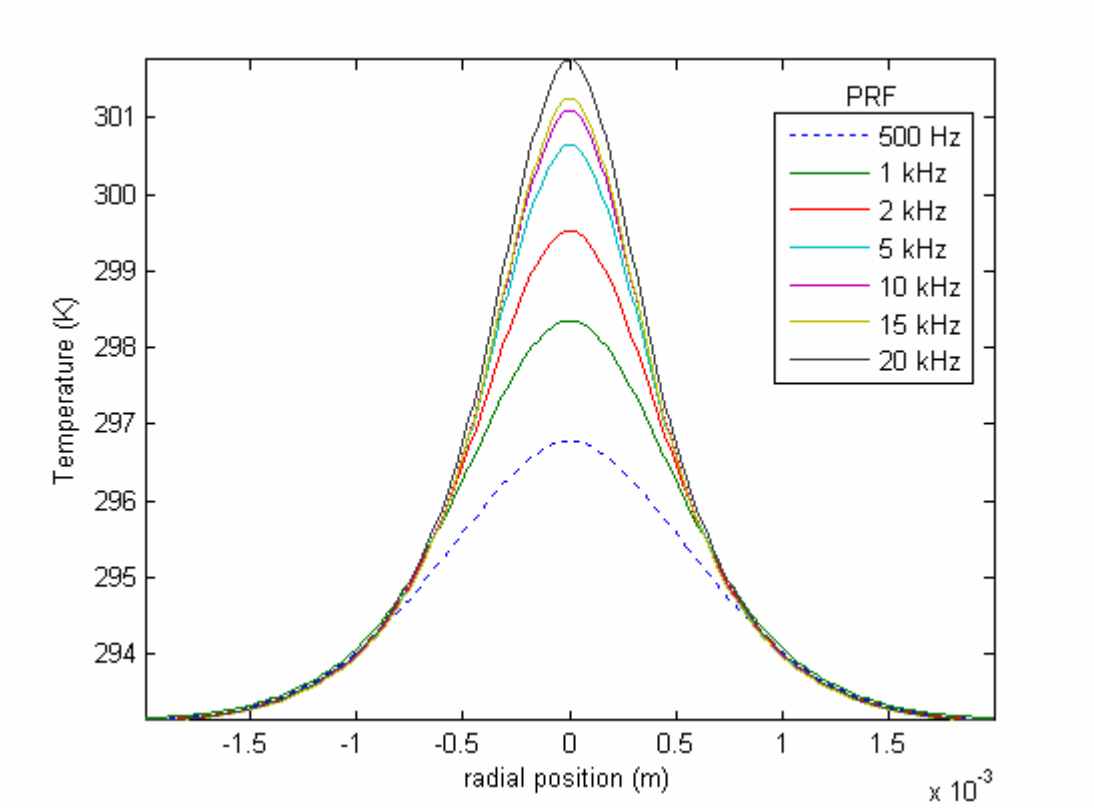

Figure 7: Radial temperature gradient for 15% duty cycle at varying PRFs.

Table 2: Thermal Lensing Power at 1 kHz PRF, 1 W peak power

PRF (kHz)	Thermal lens power (m^{-1})
0.5	1.40
1	2.43
2	3.60
5	4.84
10	5.37
15	5.59
20	5.97

5. Conclusions

Time-dependent modeling of thermal effects in laser materials is a viable option for understanding the influences of laser parameters such as PRF and duty cycle on laser performance. The model agrees well with experimental results for the chopped pumping case but does not directly agree with Q-switched pumping because the time delay between absorption and heat transfer to the host material is not accounted for in our model. Future modeling work will focus on clarifications of the chopped laser results and on development of a way to model the time delay between Q-switched pumping and heating of the host material.

Acknowledgements

This work was supported by the Air Force Office of Scientific Research and the Sensors Directorate, Air Force Research Lab.

References

[1] L. D. DeLoach, R. H. Page, G. D. Wilke, S. A. Payne, and W. F. Krupke, “Transition metal-doped zinc chalcogenides: spectroscopy and laser demonstration of a new class of gain media,” IEEE J. Quantum Electronics **32**(6), 885-895 (1996).

[2] U. Hömmerich, X. Wu, and V. R. Davis, “Demonstration of room-temperature laser action of 2.5 μm from Cr^{2+}:$Cd_{0.85}Mn_{0.15}Te$,” Optics Letters **22**(15), 1180-1182 (1997).

[3] J. B. McKay, K. L. Schepler, and G. C. Catella, “Efficient grating tuned mid-IR Cr^{2+}:CdSe laser,” Optics Letters **24**(22), 1575-1577 (1999).

[4] P. A. Berry, "Thermal Lens Mitigation and Modeling of Chromium-doped Zinc Selenide Laser Sources," Thesis, School of Engineering, University of Dayton, Dayton, OH (2005).

[5] R. D. Peterson and K. L. Schepler, "1.9 micron-Fiber-Pumped Cr:ZnSe Laser," in *Advanced Solid-State Photonics 2005 Technical Digest on CD-ROM* (The Optical Society of America, Washington, DC 2005), MB13.